

Quantitative velocity measurement in thin-gap Poiseuille flows

Dana Ehyaei¹ and Ken T Kiger¹

¹ Department of Mechanical Engineering, University of Maryland, College Park, Maryland
ehyaei@umd.edu, kkiger@umd.edu

INTRODUCTION

The current work is focused on making quantitative velocity measurements with a large field-of-view within a thin-gap planar channel. Such flows would be commonly encountered in microfluidic systems when desiring to examine a large region of the device (rather than in a single channel), or for making measurements in Hele-Shaw cells, which is a planar thin-gap device often used as an analog for flow within a porous medium. In contrast to a standard PIV measurement (where a thin light sheet is used to limit the depth of the interrogation region), thin-gap flows are typically volumetrically illuminated and a narrow depth of focus objective lens is usually employed to provide a “depth of influence” and hence set the thickness of the interrogation region [1,2]. While this works well for a small field-of-view conditions where a small depth-of-focus relative to the channel depth can be maintained using a high-magnification objective, it is impossible for a large field of view, as the magnification must necessarily be decreased. One example of such a flow is convection within a Hele-Shaw cell where a large field of view is necessary for observing the full evolution of the flow pattern. Such cases inspire our current efforts to quantify the effect of velocity and particle concentration variation due to the presence of significant velocity gradient in the wall-normal direction (Figure 1).

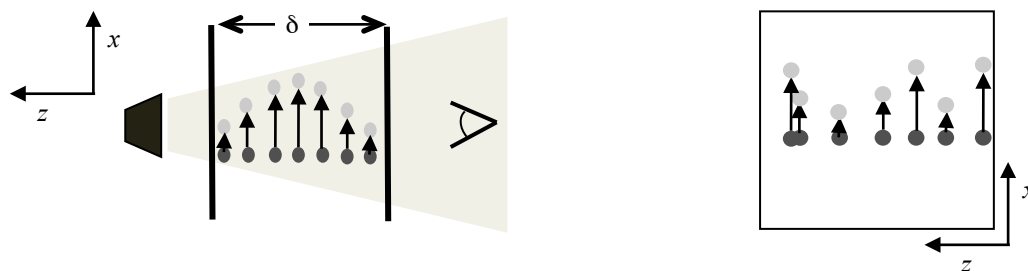


Figure 1 A volumetrically illuminated narrow channel (left), schematic of a single velocity distribution due to random location of particles across the gap (right)

As mentioned above, the main difficulty in making quantitative measurements lies in the effects caused by the strongly non-uniform velocity gradient that exists across the gap, and the potential bias caused by the migration of particles in the wall-normal direction. This point has been recently documented and outlined by Roudet et al [3], who demarked the possible flow conditions on the basis of a viscous diffusion time, $T_p = (\delta/2)^2/\nu$ (δ is the gap width and ν the kinematic viscosity), and a particle migration time, $T_m = 2.66\pi z_{eq} \delta^3/V Re_c a^3$ (V is the gap-averaged velocity, z_{eq} is the migration equilibrium position, a is the particle radius, and $Re_c = V\delta/\nu$), into 3 possible regimes:

- 1) Case I: at short times when $t \ll T_p$, the flow across the width of the gap is still uniform, and the PIV measurement unambiguously returns this value
- 2) Case II: when $t \ll T_m$, the migration of the particles has not had time to develop, regardless of the flow development
- 3) Case III: $t > T_m$ and $t > T_p$, implying that the particles have migrated to their equilibrium positions, and so the PIV measurement returns a velocity corresponding to the value given by the equilibrium position in the wall-normal Poiseuille profile.

The current work is focused on clarifying and quantifying the details associated with conducting experiments for conditions described by Case II and III. In what follows, we first examine the effect of the non-uniform Poiseuille flow in the presence of a uniform concentration, followed by a subsequent accounting for the transient evolution of the particles. In the final section we discuss recommendations on various means to attain Case III conditions, and present a simple example case of utilizing this in a practical flow.

RESULTS AND DISCUSSION

Both PIV experiments and numerical simulations of a simple fully developed Poiseuille flow were conducted to quantitatively describe the effects of the non-uniform velocity and concentration on the correlation function. We will first examine the case II conditions where particles were uniformly scattered across the gap, followed by the conditions leading to case III where the particles migrate partially or completely towards their equilibrium position.

The experiments were conducted using vertically oriented Hele-Shaw cell. The gap was formed by two rectangular tempered glass plates, 1.27 cm thick, a U-shaped shim spacer with a known thickness (varying between 0.2 to 1 mm), and a supporting frame. Glass plates were chosen to provide optical access through the device, and also to avoid any gap thickness uncertainty due to buckling of the walls. The spacer was pressed between the plates by the steel frame, with a bolt spacing of 5 cm on the sides to ensure a uniform compression and a constant gap thickness. A single inlet was fabricated for a precision syringe pump to provide the device with a steady flow at the bottom while the top boundary remained open. To decrease potential for particle migration in the feed system and manifold, a relatively short (125 mm) flexible tube (3mm ID) was used for connecting the pump to the device. Gap based Reynolds numbers were ranged between $0.7 < Re_c < 15$ for all experiments.

Monodisperse Polystyrene microspheres with a typical diameter of 15 μm and a standard deviation of less than 1.1 μm were used as tracer particle. These particles were nearly neutrally buoyant (1.05 SPG), and remained well dispersed in water. A camera (1080 x 1920 pixels, 10 μm pixel size) recorded images of a 34 x 60 mm region using a zoom lens ($f\# = 8$) while a 600 W halogen light with a Fresnel collimating lens was placed approximately 2 m away on the far side of the Hele-Shaw cell, providing a uniform oblique forward scatter illumination of the entire flow volume. The depth of field of the system was set larger than the channel gap spacing so that the tracer particles across the entire gap were mapped identically in the image plane.

Synthetic PIV images of a fully developed Poiseuille flow were generated using a Gaussian particle intensity distribution that was discretized to a uniform grid by assigning a pixel intensity corresponding to the amount of energy received by a given pixel. For simplicity, no noise was added to the background and a uniform particle diameter was used within a given test. Initial simulations were conducted with particles scattered uniformly across the depth of the gap. For migrating flows, the analytical results of Ho and Leal [4] were used to calculate the trajectory of individual tracer particles as they moved through the cell, allowing for a realistic and gradual migration to be observed.

Effect of non-uniform velocity with uniform concentration

The large variation in the displacement distribution due to sampling the variation of velocities across the gap results in a bias of the of flow velocity probability distribution function (PDF), as shown in Figure 2. For a PIV interrogation, the correlation function is often modeled as a convolution of the velocity PDF, the autocorrelation of the particle images, and a random noise component due to the limited number of particle samples within the interrogation volume [5,6]. For an ensemble correlation interrogation of the flow (or conditions where a very large number of particles existing within the interrogation window), this results in a correlation function that has a peak that is smeared out due to the variation of the velocity PDF (see Figure 2). Given these conditions, one would predict that the location of the correlation peak will represent the maximum velocity in the gap, as suggested by prior studies on the effect of velocity gradients on the correlation function [6,7]. Both our experiments and numerical simulations confirm this fact, which is in contrast to the observations given by Roudet et al [3], who reported that their measurements gave the gap-averaged velocity ($U_{piv} = 2V_{max}/3$), and not the peak value. We believe this discrepancy to be due to the fact that were observing the effect of the early stages of particle migration, and that a much more stringent criteria for the particle migration time should be used to determine the boundary of the case II conditions. Details on this particular point will be discussed in the next section, which addresses the effect of non-uniform particle concentration.

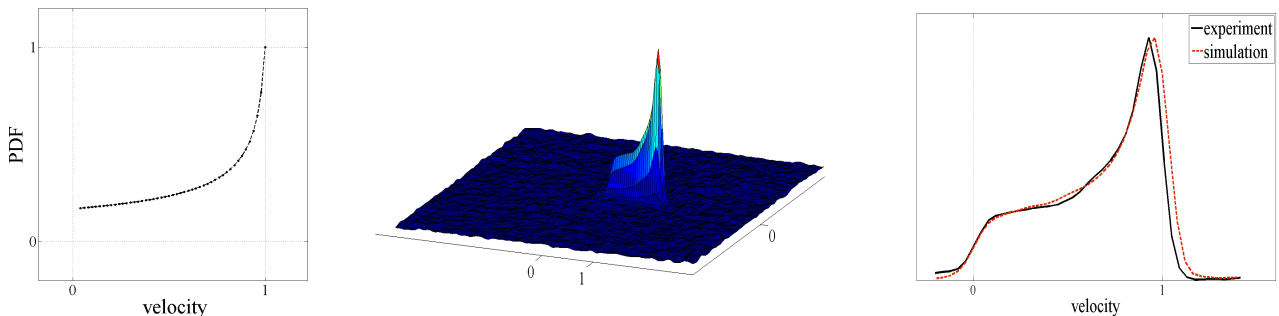


Figure 2 Velocity PDF (left), ensemble average of correlation maps (center), middle slice of averaged map (right). The velocity is normalized by the peak centerline velocity.

In addition to early stages of particle migration, the particle image size and the particle image density will also have a significant effect on the bias and random errors associated with a PIV interrogation. The particle size is directly relevant due to the fact that the correlation is effectively a convolution of the particle image with the velocity probability distribution function. A small particle image size in comparison to the maximum displacement will provide the most accurate representation of the velocity PDF, due to the minimal distortion this creates to velocity PDF. The larger the particle size in comparison to the maximum displacement, the greater the distortions of the PDF, introducing a bias shift in the effective peak location. This effect is summarized in Figure 3, which reports the ensemble correlation peak location for a range of particle image sizes (d/D_I , where the particle image size, d , is normalized by the interrogation window size) and maximum displacement ($\Delta x_m/D_I$). For the largest displacement (black line with circle symbols, $\Delta x_m/D_I = 0.24$), the bias tends towards zero for the smallest particles sizes, and increases to just over 30% for a particle with an image diameter that is close to half the interrogation window size. Conversely, for small displacements (such as $\Delta x_m/D_I = 0.03$ or smaller, corresponding to a 2 pixel displacement in a 64 pixel interrogation window), the bias error is such that the true peak is underestimated by 20 to 30% for all particle sizes.

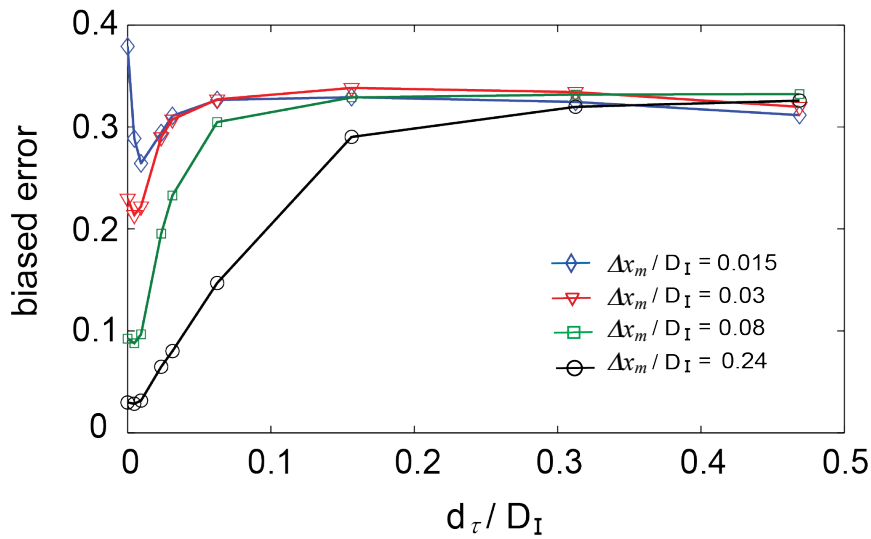


Figure 3 PIV displacement estimate biased error, $\epsilon_{\text{biased}} = (\Delta x_{\text{true}} - \Delta x_{\text{piv}}) / \Delta x_{\text{true}}$ as a function of particle image size d , and maximum displacement, Δx_m (normalized with interrogation window size, D_I), for uniform tracer particle concentration.

The above consideration of particle image size neglected the influence of random correlation noise due to a small image particle density, N_I . The random correlation component is a well documented and important effect in uniform displacement flows, and has led to the standard recommendation guideline of maintaining approximately 8 to 10 particles images in an interrogation region to ensure a yield of 95% valid vectors [8,9]. The highly non-uniform velocity PDF greatly increases this requirement to ensure that the interrogation peak is

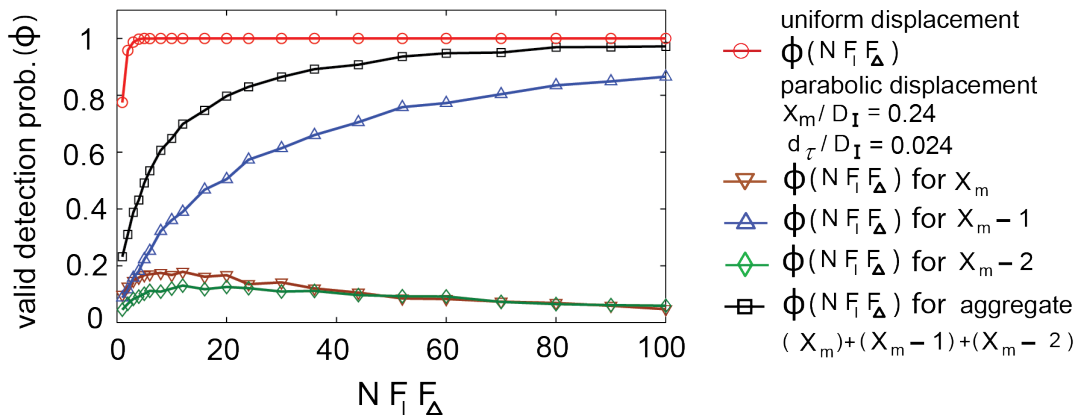


Figure 4 Valid detection probability for the displacement correlation peak as a function of the effective number of particle images within an interrogation window ($N_{F_1 F_A}$) for $F_o = 1$. Note that three expected peak locations are tracked near the maximum displacement, and compared to the results of a uniform displacement (shown in red).

likely to occur at a known and repeatable position near the maximum displacement expected by a well-converged correlation. The numerical simulations were used to quantify the likelihood of a valid detection from a single interrogation depending on the effective image density, $N_I F_I F_s$, the results of which are shown for the case of $\Delta x_m / D_I = 0.24$ and $d / D_I = 0.02$ in Figure 4. The most likely peak location for these conditions was 1 pixel less than the peak displacement ($\Delta x_m - 1$) due to the particle size bias effects mentioned above. Even so, including approximately 100 particles within the interrogation window produced only an 83% probability of making a valid measurement. If one were to consider the neighboring positions of Δx_m and $(\Delta x_m - 2)$ as a “valid” measurement, this would increase to approximately 94%. This does not give one confidence in making a very reliable measurement under these conditions, as one must sacrifice considerable spatial resolution to attain such a high effective seeding density. These simulations are also optimistic, in that effects of sensor noise and particle non-uniformities are not accounted for, which would further decrease the probability of a valid measurement. Results for simulation of a uniform displacement for all particles are shown in the figure for comparison.

Effect of non-uniform tracer uniform concentration

In addition to the direct influence of the wall-normal velocity gradient, the correlation peak is also influenced by any nonuniform distribution of tracer particles across the gap. Indeed, in small depth-of-focus systems, its influence has been used to extract both velocity and concentration profiles [4]. Previous studies have shown that neutrally buoyant rigid spheres undergo a wall-normal migration away from both of the walls and the center plane of the channel in Poiseuille velocity profile, reaching an equilibrium position across the gap [5]. Similarly migration of tracers creates an evolving non-homogeneity in their spatial distribution across the gap, which once again results in a sample bias of the PDF of flow velocity in each interrogation window. To observe this effect experimentally, tests were performed for several non-dimensional stream-wise locations ($x' = x/X$, where $X = v\delta^3 / V_{max}a^3$, where V_{max} is the maximum velocity at the center of the channel). For each individual test, the images were interrogated and the evolution of ensemble average correlation peak was studied. Figure 5 shows the results of the experiment, along side results produced from synthetic images of tracer particles migrating according to the theory of Ho and Leal [4].

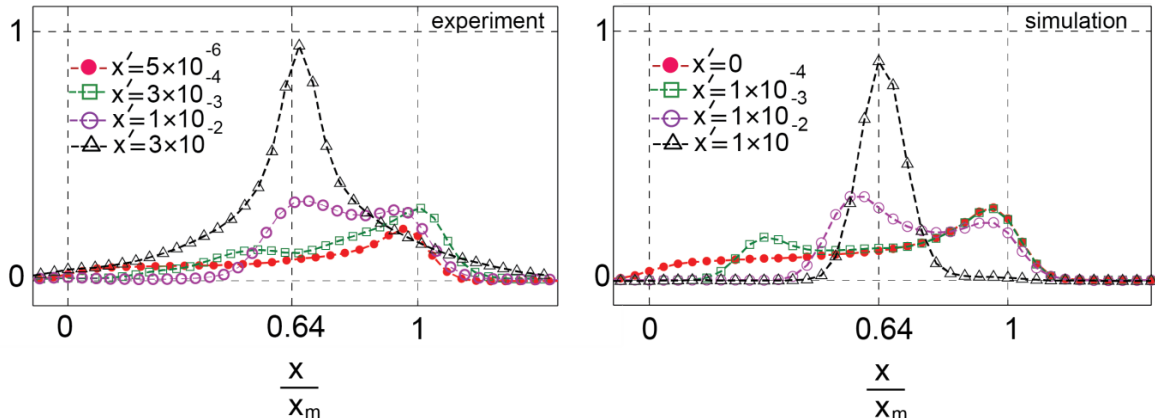


Figure 5 Normalized averaged correlation functions, experimental (left) and simulation (right).

Starting from a homogeneous concentration distribution, a broad correlation function with the highest peak corresponding to maximum velocity across the gap is predicted. However the correlation function starts to evolve as particles begin to migrate across the channel, thus providing a bias sampling of the velocity distribution. A second peak emerges as the particles rapidly move away from the wall, as observed around $x' \sim O[10^{-4}]$. As tracers subsequently migrate from the center plane as well, the two peaks eventually merge into a single sharp and relatively high peak. This happens when most of the tracers are packed at their stable position. Downstream of this position, the correlation remains unchanged, with a peak value that would predict $U_{piv} = 0.64V_{max}$.

Presence of multiple peaks and evolving peaks within the expected correlation function makes the probability of choosing a reliably meaningful displacement even less likely than noted when combined with the particle image size effects and random correlation noise. This then would tend to render PIV measurements under such conditions to being qualitative unless one can ensure sufficient evolution to the point where the particles have reached their segregated state, corresponding to $x' \sim O[10^{-2}]$. In our own experience, this can be done through careful manipulation of the inflow geometry or filling conditions. We have conducted experiments where the Hele-Shaw cell was designed with an extra length section to provide sufficient development length during filling to ensure full segregation. Alternatively, if a longer filling length could not be accommodated, generating an oscillatory within the gap could be used to drive the particles toward their equilibrium position by using numerous short strokes in alternating directions (provided the

Womersley number was kept small enough to ensure a quasi-steady parabolic profile). Finally, work of Mielnik and Saetran (2006) could also be adapted for this purpose, who introduced selective seeding of thin particle “sheets” into their channel by manipulating the flow through a series of T-junction inflow channels, confining the particle laden flow to a specific cross-gap location. All of these solutions would allow for use of standard uniform PIV displacements, and hence take advantage of the demonstrably improved accuracy and resolution that is possible under uniform displacement conditions.

REFERENCES

- [1] Meinhart C, Wereley S, Santiago J, “PIV measurements of a microchannel flow” *Exp. Fluids* 27:414–19 (1999)
- [2] Kloosterman A, Poelma C, Westerweel J, “Flow rate estimation in large depth-of-field micro-PIV” *Exp. Fluids* 50:1587-1599 (2011)
- [3] Roudet M, Billet A-M, Risso F and V Roig, “PIV with volume lighting in a narrow cell: An efficient method to measure large velocity fields of rapidly varying flows” *Exp. Them. Fluid Sci.* 35:1030-1037 (2011)
- [4] Ho B, Leal L, “Inertial migration of rigid spheres in two-dimensional uni-directional flows” *JFM.* 65, 365 (1974)
- [5] Olsen MG and RJ Adrian, “Out-of-focus effects on particle image visibility and correlation in microscopic particle image velocimetry,” *Exp. Fluids*, [Suppl.] S166-S174 (2000)
- [6] Wereley ST and Whitacre I, “Particle dynamics in a dielectrophoretic microdevice,” in *BioMEMS and Biomedical Nanotechnology* (series ed M. Ferrari): Vol. 4: Biomolecular Sensing, Processing and Analysis (vol. eds R. Bashir and S.T. Wereley), Kluwer, Boston (2007)
- [7] Westerweel J, “On velocity gradients in PIV interrogation” *Exp Fluids.* 44:831-842 (2008)
- [8] Keane RD and RJ Adrian, “Theory of cross-correlation analysis of PIV images,” *Appl. Sci. Res.* 49:191-215 (1992)
- [9] Adrian RJ and J Westerweel, *Particle Image Velocimetry*, Cambridge University Press, London (2011)
- [10] Mielnik MM and LR Saetran, “Selective seeding for micro-PIV,” *Exp. Fluids*, 41: 155-159 (2006)